ЖЭТФ/JETP, 2027, том 171, вып. 1, стр. 18–24 © 2027

NONLINEAR TUNNEL OSCILLATIONS OF LIGHT IN SPHERICAL BRAGG RESONATORS

V. P. Ruban*

L. D. Landau Institute for Theoretical Physics of the Russian Academy of Sciences
142432, Chernogolovka, Moscow region, Russia

Received September 1, 2026,
revised version September 1, 2026
Accepted for publication October 27, 2026

A weakly nonlinear regime of radial tunneling is theoretically considered for a light wave in a spherical dielectric Bragg resonator containing a set of "shell" eigenmodes (both TE and TM) with different azimuthal numbers $l \geqslant 1$, which are concentrated near a defect of the Bragg structure, several layers away from the origin. Also, a single mixed radial mode with $l = 1$ is located near the resonator center, either TM or TE. In the main approximation, the Kerr nonlinearity is relevant for the central mode only, while all the shell modes remain in the linear regime. The tunneling occurs between the central mode and the shell $l = 1$ mode of the same symmetry. The nontrivial part of the dynamics of the optical field is described by a Hamiltonian system of ordinary differential equations for complex vectors $\mathbf{C}_1(t)$ and $\mathbf{C}_2(t)$, which determine the magnitude and spatial orientation of the wave structures at the center and at the shell, respectively. Depending on the "asymmetry parameter" of tunnel coupling, the system demonstrates different variants of nonlinear behavior.

Keywords: spherical Bragg resonators, tunnel oscillations, Kerr nonlinearity

DOI: 10.31857/S0044451027010022

1. INTRODUCTION

Wave tunneling is a fundamental phenomenon observed in many fields of physics. As is known, when a weak coupling between two resonators with nearly equal eigen-frequencies takes place, tunnel oscillations are possible in such a wave system. For instance, in quantum mechanics in the simplest case the wave is of scalar type, the motion is one-dimensional, and the resonators are potential wells [1]. For optics, however, the case of a vectorial wave in three-dimensional space is more important. Such problems are technically more complicated (see, e.g., [2–8]). In particular, the light can be localized on defects of some photonic crystals (if the forbidden band exists there) and tunnel between such modes (see, e.g., [9–14], and references therein). In this connection, of special interest are dielectric layered structures with spherical symmetry, where the radial confinement of light is realized through the Bragg reflection, and complete linear analysis is easy to perform due to separation of variables (see [15–18], and references therein). By a properly designed profile of dielectric permittivity $\varepsilon(r, \omega)$, it is possible to realize close frequencies for trapped states concentrated near defects of the r-periodic structure. In this case, the eigen-frequencies fall into the forbidden band of radial motion.

In the linear approximation, such dielectric spherical Bragg resonators have been well studied, especially for the cases where the permittivity profile $\varepsilon(r, \omega)$ is a piecewise constant function of radial coordinate r at fixed frequency ω [16–18]. However, nonlinear effects definitely require more attention. The purpose of this work is to take into account nonlinearity of Kerr type in the dynamics of tunnel oscillations of light, when two weakly coupled radial modes corresponding to the azimuthal number $l = 1$ are present, one of them being located near the resonator center, while the other mode occupying a "shell" several (about 10–20) layers away. A system of ordinary differential equations (ODE) will be derived here for simplified description of tunneling processes. Vectorial nature of light will be seen to fully manifest itself in such system, particularly in the structure of nonlinear interaction. Due to a quite small relative difference between the two eigen-

* E-mail: ruban@itp.ac.ru

frequencies, even a low intensity of the optical field will be able to introduce strong nonlinear effects. A "parameter of asymmetry" will appear in the ODE system, describing the relationship between the true eigen-modes and their more localized linear combinations. That parameter will make an additional contribution to a rich variety of nonlinear dynamical regimes. Besides fundamental scientific interest, the results obtained here can be useful for optical technologies.

2. STRUCTURE OF EIGEN-MODES

Let us first recall some necessary facts from the linear theory. We consider a locally isotropic, spatially nonuniform dielectric medium (with temporal dispersion, but without spatial dispersion) in its "transparency window" [19]. In other words, the imaginary part of dielectric permittivity in the frequency range of our interest is negligibly small (of course, it is not small outside the transparency window, i.e., in absorption bands). For practical applicability of results obtained in this work, the condition $\operatorname{Im}\varepsilon \lesssim 10^{-4}$ is required, as will be clear from the further consideration. It is not restrictive, since the absorption of light can be actually much weaker, for example in glass.

Thus, in a sufficiently wide frequency interval near some ω_0, we adopt the model of a perfect dielectric with no material losses. Since the Kramers–Kronig relations must necessarily be satisfied, $\varepsilon(r,\omega)$ is a nontrivial real positive function at real ω in the indicated domain, with inequality $\partial\varepsilon/\partial\omega > 0$ taking place [19].

With the above assumptions, in the linear approximation the problem is reduced to finding spatially localized solutions of the vector equation for the complex amplitude of (monochromatic) electric field,

$$\operatorname{rot}\operatorname{rot}\mathbf{E} = \frac{\omega^2}{c^2}\varepsilon(r,\omega)\mathbf{E}. \tag{1}$$

Two types of eigen-modes exist (see, e.g., Ref. [15]). Transverse-electric (TE) modes have the form

$$\mathbf{E}_{\mathrm{TE}} = \Psi(r)[\nabla_{\mathbf{n}} Y_{l,m}(\mathbf{n}) \times \mathbf{n}], \tag{2}$$

where $Y_{l,m}$ is a spherical harmonic, $\mathbf{n} = \mathbf{r}/r$ is the unit vector, and a radial function $\Psi(r)$ satisfies the equation

$$-\Psi'' - \frac{2}{r}\Psi' + \frac{l(l+1)}{r^2}\Psi - \frac{\omega^2}{c^2}\varepsilon(r,\omega)\Psi = 0. \tag{3}$$

For transverse-magnetic (TM) modes, the following equality takes place,

$$\frac{c^2}{\omega^2}\operatorname{rot}\mathbf{E}_{\mathrm{TM}} = F(r)[\nabla_{\mathbf{n}} Y_{l,m}(\mathbf{n}) \times \mathbf{n}], \tag{4}$$

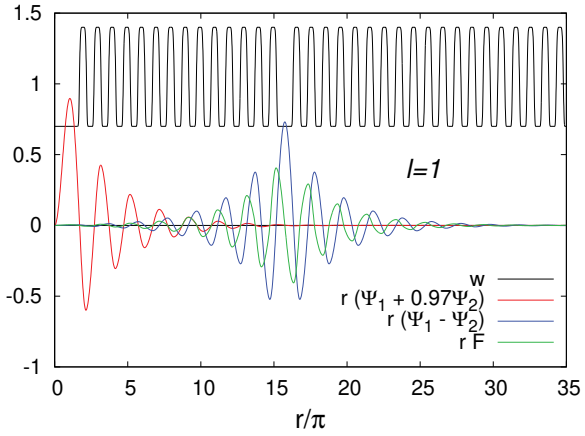

Fig. 1. Examples of localized (non-normalized) linear solutions in the presence of central TE-mode. Here 14 layers with larger dielectric permittivity are arranged at intervals of π starting from coordinate $r_0 = 1.938\pi$, and all the other layers are additionally shifted along r by 0.612π. The eigen-frequencies are $\xi_1 = -0.00066164155$, $\xi_2 = 0.001185237$. Also, the shell mode of TM type is shown, for which $\xi_{\mathrm{TM}} = 0.0002669188$

so that the electric induction $\varepsilon(r,\omega)\mathbf{E}_{\mathrm{TM}}$ is given by the formula

$$\varepsilon\mathbf{E}_{\mathrm{TM}} = l(l+1)\frac{F(r)}{r}\mathbf{n}Y_{l,m}(\mathbf{n}) + \frac{d}{rdr}[rF(r)]\nabla_{\mathbf{n}}Y_{l,m}(\mathbf{n}). \tag{5}$$

The equation for function $F(r)$ is somewhat different from Eq. (3):

$$-F'' - \frac{2}{r}F' + \frac{l(l+1)}{r^2}F + \frac{\varepsilon'}{\varepsilon r}\frac{d}{dr}(rF) - \frac{\omega^2}{c^2}\varepsilon F = 0, \tag{6}$$

where $\varepsilon' = \partial\varepsilon/\partial r$.

In our case, the permittivity $\varepsilon(r,\omega)$ behaves periodically in r at large distances from the origin. Therefore differential equations for functions $\psi(r) = r\Psi(r)$ and $f(r) = rF(r)$ contain in that region the only non-periodic coefficient $l(l+1)/r^2$, and it is negligibly small with moderate values of l. For such equations, a gap in the frequency spectrum (the forbidden band) is known to exist. When ω is inside the gap (the Bragg regime), the general solution is a sum of two oscillatory functions with non-uniform amplitudes, one of them exponentially growing and the other exponentially decaying.

We are interested in regular solutions $\Psi(r)$ and $F(r)$ which at small $r \ll c/\omega_0$ behave as r^l, while at $r \to +\infty$ they tend to zero. In the Bragg regime, the amplitude of their oscillations approaches zero at large r exponentially fast (see examples in Figs. 1 and 2). Within the transparency window, such bound states exist for some special discrete (non-degenerate) real values of frequency only, when the coefficient in front of the

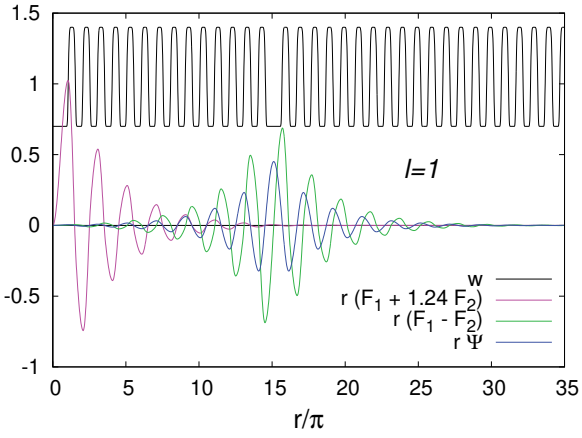

Fig. 2. Examples of localized (non-normalized) linear solutions in the presence of central TM-mode. Here 14 layers with larger dielectric permittivity are arranged at intervals of π starting from coordinate $r_0 = 1.302\pi$, and all the other layers are additionally shifted along r by 0.62π. Here the eigen-frequencies are $\xi_1 = -0.0023929839$, $\xi_2 = -0.0001324124$. Also, the shell mode of TE type is shown, for which $\xi_{\rm TE} = -0.0013708785$

growing exponent takes zero value. Since the eigen-modes $\Psi(r)$ and $F(r)$ are determined up to an arbitrary multiplier, they can be taken purely real without limitation of generality. Numerically, these functions can be found by standard methods very easily. In particular, the "shooting" method works quite accurately.

We should say that it was the neglect of material losses that allowed us to avoid many difficulties related to the complexity of eigen-frequencies in the general case. Another important point is that radiative losses can be considered as negligibly small for a large but finite size $R_{\max}$ of the Bragg structure due to the exponential decay of the modes at large r. Practically, a maximal radius of several tens of wavelengths is quite enough. If necessary, small material and radiative losses can be included into the analysis via a perturbative procedure.

3. QUASI-MONOCHROMATIC APPROXIMATION

In this work, we will deal with modes having eigen-frequencies near ω_0. Therefore it will be convenient to normalize the time variable t by factor $1/\omega_0$, and the radial coordinate r by factor $c/\omega_0\sqrt{\bar\varepsilon}$, where $\bar\varepsilon$ is a value of dielectric permittivity somewhere in the middle of the range between its minimum and maximum in the r-periodic profile at ω_0. We stress that any linear combination of such modes is quasi-monochromatic in the frequency range, but not in the wave-vector space. Indeed, the spatial Fourier spectrum of each mode is rather wide.

The crucial simplification in our further analysis will be achieved through expansion of function $\omega^2\varepsilon(r,\omega)$ up to the first order in the small deviation $\xi = (\omega/\omega_0 - 1)$, so that

$$\frac{\omega^2\varepsilon(r,\omega)}{\omega_0^2\bar\varepsilon} \approx w(r) + \tau(r)\xi. \qquad (7)$$

Since ω_0 is assumed to lie in a transparency window of dielectric medium, functions $w(r)$ and $\tau(r)$ are purely real and strictly positive. Moreover, $\tau(r) > 2w(r)$ by virtue of the inequality $\partial\varepsilon/\partial\omega > 0$ [19]. So, approximation (7) reduces Eq. (1) to a more or less standard self-adjoint problem for eigen-values and eigen-modes.

For numerical examples presented later, we used the expression

$$w(r) + \tau(r)\xi = 0.7 + 1.5\xi + \\ + \sum_j (0.7 + 1.7\xi)\exp[-4.0(r - r_j)^6], \qquad (8)$$

where the array of positive numbers r_j determines radial coordinates of middles of layers with higher dielectric permittivity. Such a smooth function to some extent approximates a layered structure with sharp boundaries between the layers. In the absence of "defects", successive values r_j differ by π, thus forming a spherical Bragg mirror, but existence of localized modes is possible only when at least one interval is different from π. The widths of such "anomalous" layers then determine the type of eigen-modes as well as their frequencies ξ_ν. By a careful choice of the intervals, all the values ξ_ν can be made quite small, in accordance with the adopted quasi-monochromatic approximation (see examples of profiles $w(r)$ with defects in Figs. 1 and 2).

In this work, the simplest case is considered when two radial modes with $l = 1$ of the same symmetry (either Ψ_1 and Ψ_2, or F_1 and F_2) are present, such that their localization is distributed between the central defect and a "shell" defect located at a distance $r_{\rm shell}$ about 10–20 layers (5–10 wavelengths) away from the origin. All the other modes are completely concentrated at the "shell" defect. Actually, such a situation is not something special, since a central defect size suitable to confine a TE mode is typically not good for trapping a TM mode, and vice versa.

It is very important that there exist such linear combinations of eigen-modes (for instance, $s_1 = S_{11}\Psi_1 + S_{12}\Psi_2$ and $s_2 = S_{21}\Psi_1 + S_{22}\Psi_2$) that one

of them is nearly completely concentrated around the center, and the other on the "shell". The concept of such a "localization matrix" $S_{\nu\mu}$ implies optimization of some properly defined "quality of localization". In the simplest case of two modes the choice of the combinations can be made roughly by eye. Just such combinations are presented in Figs. 1 and 2. Recalling the famous example with two potential wells from quantum mechanics, we clearly see here a direct analogy between the "one-well" states and our "mixed" functions s_1, s_2. With proper normalization, as will be shown later, matrix $S_{\nu\mu}$ is orthogonal,

$$S_{\nu\mu} = \frac{1}{\sqrt{1+a^2}} \begin{pmatrix} 1 & a \\ a & -1 \end{pmatrix}, \tag{9}$$

where a is an "asymmetry parameter" depending on the dielectric permittivity profile. Therefore coefficients $c_1(t)$ and $c_2(t)$ in the expression for the radial mode (with fixed number m),

$$\Psi_{\rm tot} e^{i\xi_1 t} = c_1 s_1 + c_2 s_2 = A_1(0)\Psi_1 + A_2(0)\Psi_2 e^{-i\Delta t}, \tag{10}$$

where $\Delta = (\xi_2 - \xi_1)$, are governed by the following system of ordinary differential equations:

$$i\dot{c}_1 = \frac{\Delta[a^2 c_1 - a c_2]}{1+a^2}, \qquad i\dot{c}_2 = \frac{\Delta[-a c_1 + c_2]}{1+a^2}. \tag{11}$$

4. EFFECT OF NONLINEARITY

It should be noted that the local intensity of light for the "central" mixed mode $s_1(r)$ is typically much larger than for $s_2(r)$ and all the other shell modes (the corresponding large factor is about $(r_{\rm shell}/\pi)^2 \sim 100$–$400$). Therefore, with moderate wave amplitudes, nonlinearity effectively acts in the central part of the resonator only. The presence of just a single central radial mode s_1 makes nonlinear analysis quite simple in comparison with the case of simultaneous existence of several central radial modes. Indeed, in our situation there will be no need to calculate terms of nonlinear cross-interactions between different central states.

To take into account effects of Kerr nonlinearity, we should go back to the basic equation

$$c^2 {\rm rot}\,{\rm rot}\,\mathbf{E}(\mathbf{r},t) = -\partial_t^2 \mathbf{D}(\mathbf{r},t) \tag{12}$$

and include into $\partial_t^2 \mathbf{D}$ the corresponding cubic terms in the quasi-monochromatic approximation [19]. As a result, we arrive at the (dimensionless) equation

$$\begin{aligned} {\rm rot}\,{\rm rot}\,\mathbf{E} = w(r)\mathbf{E} + i\tau(r)\partial_t \mathbf{E} + \\ +\alpha(r)|\mathbf{E}|^2\mathbf{E} + \beta(r)(\mathbf{E}\cdot\mathbf{E})\mathbf{E}^*, \end{aligned} \tag{13}$$

where $\alpha(r)$ and $\beta(r)$ are (real) Kerr coefficients, and $\mathbf{E}^*$ is the complex conjugate vector.

It is important that Eq. (13) represents a non-canonical Hamiltonian system

$$i\tau(r)\partial_t \mathbf{E} = \delta\mathcal{H}/\delta\mathbf{E}^*, \tag{14}$$

with the Hamiltonian functional

$$\mathcal{H} = \mathcal{H}^{(2)} + \mathcal{H}^{(4)},$$

where

$$\mathcal{H}^{(2)} = \int \Big[|{\rm rot}\,\mathbf{E}|^2 - w(r)|\mathbf{E}|^2\Big] d\mathbf{r}, \tag{15}$$

$$\mathcal{H}^{(4)} = -\int \Big[\frac{\alpha(r)}{2}|\mathbf{E}|^4 + \frac{\beta(r)}{2}|(\mathbf{E}\cdot\mathbf{E})|^2\Big] d\mathbf{r}. \tag{16}$$

In this case any two eigen-functions of linear approximation with differing frequencies automatically turn out to be mutually orthogonal, if the scalar product is defined by the following formula:

$$\langle 1|2\rangle = \int \tau(r)(\mathbf{E}_1^*\cdot\mathbf{E}_2) d\mathbf{r}. \tag{17}$$

The angular dependences through $Y_{l,m}$ ensure the orthogonality also for $(2l+1)$-fold degenerate states with definite l. At $l=1$, it will be convenient for us to use real functions $(\mathbf{e}_k\cdot\mathbf{n})$ as the angular multipliers, where $k = \{x,y,z\}$.

Tunnel processes are better studied in terms of the previously introduced functions s_1 and s_2 (or analogous mixed modes in the case of TM states). In view of orthonormality of the eigen-modes, the corresponding transformation matrix $S_{\nu\mu}$ can be taken orthogonal, which fact was mentioned earlier. In particular, for TE modes the summed electric field is expressed as

$$\mathbf{E}_{\rm TE} e^{i\xi_1 t} = [\mathbf{C}_1(t)\times\mathbf{n}]s_1(r) + [\mathbf{C}_2(t)\times\mathbf{n}]s_2(r), \tag{18}$$

and functions $s_\nu(r)$ are normalized as follows:

$$\frac{8\pi}{3}\int_0^\infty \tau(r) s_\nu^2(r) r^2 dr = 1. \tag{19}$$

It is implied that the forbidden band in the frequency spectrum is much wider than Δ (with the permittivity profile corresponding to Eq. (8), we have $\Delta/\Delta_{\rm gap} \sim 0.01$). In such a situation, nonlinear interaction between trapped modes and continuous spectrum is much weaker than between the confined states. Therefore, if the vectors $\mathbf{C}_{1,2}$ are both of the same order and sufficiently small, then nonlinearity does not introduce essential distortions into expression (18), but it

just modifies the equation of motion for the coefficient $\mathbf{C}_1(t)$ compared to the linear regime. In contrast, the shell-mode amplitude $\mathbf{C}_2(t)$ is not affected directly by the nonlinearity by virtue of the smallness (by a factor $\sim \pi/r_{\rm shell}$) of the electric field there in comparison with the central mode. The other shell modes with different l remain in the linear regime as well, and thus they do not participate in the dynamics.

Nonlinear corrections can be easily calculated by the variational method through the Lagrangian structure of Eq. (13) and orthogonality of modes s_1 and s_2. It is sufficient to substitute (18) into expression (16), and thus obtain

$$H^{(4)} = -\frac{\tilde{\alpha}}{2}|\mathbf{C}_1|^4 - \frac{\tilde{\beta}}{2}|(\mathbf{C}_1\cdot\mathbf{C}_1)|^2, \qquad (20)$$

where the new effective Kerr coefficients

$$\tilde{\alpha} = (7I_\alpha + 2I_\beta), \quad \tilde{\beta} = (I_\alpha + 6I_\beta)$$

are expressed through the integrals

$$I_\alpha = \frac{4\pi}{15}\int\limits_0^\infty \alpha s_1^4 r^2 dr, \quad I_\beta = \frac{4\pi}{15}\int\limits_0^\infty \beta s_1^4 r^2 dr. \qquad (21)$$

As a result of substitution of the variational ansatz (18) into the corresponding Lagrangian functional

$$\mathcal{L} = i\int \tau(r)(\mathbf{E}^*\cdot\partial_t\mathbf{E})d\mathbf{r} - \mathcal{H},$$

the equations of motion for vectors $\mathbf{C}_1$ and $\mathbf{C}_2$ take the form

$$i\dot{\mathbf{C}}_1 = \frac{\Delta}{1+a^2}[a^2\mathbf{C}_1 - a\mathbf{C}_2] - \\ -\tilde{\alpha}|\mathbf{C}_1|^2\mathbf{C}_1 - \tilde{\beta}(\mathbf{C}_1\cdot\mathbf{C}_1)\mathbf{C}_1^*, \qquad (22)$$

$$i\dot{\mathbf{C}}_2 = \frac{\Delta}{1+a^2}[-a\mathbf{C}_1 + \mathbf{C}_2]. \qquad (23)$$

An analogous system of ODE (but with different expressions for parameters $\tilde{\alpha}$ and $\tilde{\beta}$) is obtained when the tunneling of TM modes is considered. We do not present here the corresponding formulas. Equations (22)–(23) constitute the main result of this work.

It is essential that with small $\Delta \sim 0.001$, nonlinearity comes into play already at quite moderate light intensities near the resonator center, corresponding to a relative nonlinear frequency shift $\delta\omega_{\rm nl}/\omega_0 \sim \alpha|\mathbf{E}|^2 \sim \Delta$. Thus, the physical limitation $\alpha|\mathbf{E}|^2 \ll 1$ is definitely satisfied.

Let us also note that passage to new variables $\tilde{t} = \Delta t$ and $\vec{C}_{1,2} = \sqrt{\tilde{\alpha}/\Delta}\,\mathbf{C}_{1,2}$ allows us to put formally $\Delta = 1$ and $\tilde{\alpha} = 1$ in system (22)–(23). As a result, only two essential parameters remain: a and $\eta = \tilde{\beta}/\tilde{\alpha}$. In the numerical examples below $\eta = 0.5$.

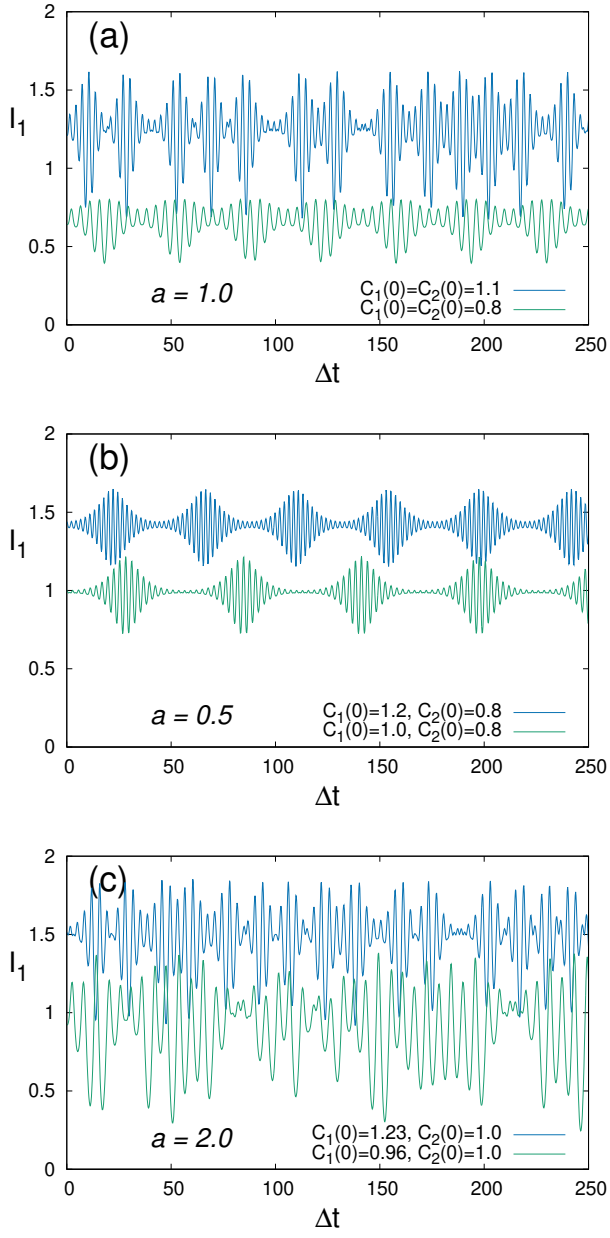

Fig. 3. Examples of various nonlinear regimes in the modelling of radial tunneling of light in the framework of equations (22)–(23)

Integrals of motion for equations (22)–(23), besides the Hamiltonian

$$H = \frac{1}{1+a^2}\times \\ \times\left[a^2|\vec{C}_1|^2 + |\vec{C}_2|^2 - a(\vec{C}_1^*\cdot\vec{C}_2) - a(\vec{C}_2^*\cdot\vec{C}_1)\right] - \\ -\frac{1}{2}|\vec{C}_1|^4 - \frac{\eta}{2}|(\vec{C}_1\cdot\vec{C}_1)|^2, \qquad (24)$$

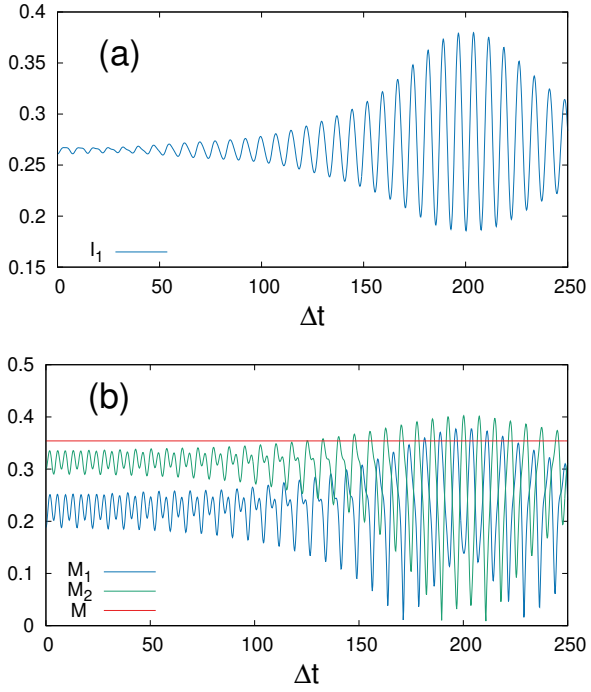

Fig. 4. Example of dynamics with non-zero total angular momentum: (*a*) burst in function $I_1(t)$; (*b*) absolute values $M_1 = |\vec{M}_1|$, $M_2 = |\vec{M}_2|$, and $M = |\vec{M}|$

are also the action (full intensity)

$$I = I_1 + I_2 = |\vec{C}_1|^2 + |\vec{C}_2|^2, \tag{25}$$

and the angular momentum

$$\vec{M} = \vec{M}_1 + \vec{M}_2 = \\ = 2[\mathrm{Re}\,\vec{C}_1 \times \mathrm{Im}\,\vec{C}_1] + 2[\mathrm{Re}\,\vec{C}_2 \times \mathrm{Im}\,\vec{C}_2]. \tag{26}$$

The presence of nonlinearity in system (22)–(23) changes the character of radial tunneling dramatically in comparison with the simple linear regime. In Fig. 3, numerical examples of temporal dependences of intensity I_1, for several values of a, are given with initial conditions in the form $\vec{C}_1(0) = (C_1(0), 0, 0)^T$, $\vec{C}_2(0) = (0, C_2(0), 0)^T$. In some cases the dynamics reveals quasi-random features. Examination has shown that exponential divergence of initially close phase trajectories takes place there, which is a typical property of dynamical chaos.

In the final example presented in Fig. 4, with $a = 2.0$, initial conditions were $\vec{C}_1(0) = (0.47, 0, 0.2i)^T$ and $\vec{C}_2(0) = (0, 0.5, 0.3i)^T$. The total angular momentum is not zero in this case, contrary to the previous examples. We observe here a kind of activity burst accompanied by exchange between the angular momenta.

5. SUMMARY

Thus, to describe the processes of radial tunneling of optical waves in purely dielectric spherical Bragg resonators, we have derived the system of ODE (22)–(23). It demonstrates various dynamical regimes, including nearly chaotic ones. The system is simpler than the analogous system in the recent work [20], where the tunneling of light between two identical potential wells with spatially distant centers was considered within a model of effectively isotropic epsilon-near-zero medium in the presence of dissipation and external pumping [21]. It was not very difficult to consider in that model also the case of a centrosymmetric potential $V(r)$ with two minima, derive the corresponding system of ODE for radial tunneling, and then compare its predictions to the results of direct three-dimensional (3D) numerical simulations. In such a way, quite good quantitative agreement has been obtained between the ODE system and the full 3D wave model. That result (not published yet) provides indirect evidence for the correctness of equations (22)–(23), since a direct numerical simulation of the 3D equation (13) seems to be quite a heavy task at the present moment. Indeed, the required numerical resolution should be as fine as 600^3 points (about 30 wavelengths along a spatial dimension, and about 20 points per wavelength). Besides that, in this case the computation should cover a long dimensionless time period of $10/\Delta \sim 10^4$.

The analysis can be generalized to the case of several ($N_s \geqslant 2$) shell modes with $l = 1$, which are concentrated at different radial coordinates. In this case, as before, the nonlinearity appears in the equation for the vector amplitude of the central mode only, but the linear part of the system is expressed through an orthogonal "localization matrix" $\hat{S}$ of size $(1 + N_s) \times (1 + N_s)$:

$$i\dot{\mathbf{C}}_\nu = [\hat{S}\,\mathrm{Diag}\{\Delta_\kappa\}\,\hat{S}^T]_{\nu\mu}\mathbf{C}_\mu + \delta_{\nu,1}[\partial H^{(4)}/\partial \mathbf{C}_1^*], \tag{27}$$

where

$$\kappa, \mu, \nu = 1, \ldots, (1 + N_s), \quad \Delta_\kappa = (\xi_\kappa - \xi_1).$$

Finally, we note that a doubtless advantage of a purely dielectric construction is its very small dissipation, so that no pumping may be needed to observe the light tunneling occurring at typical time intervals like 10^4 wave periods.

Funding. This work was supported by the Ministry of Science and Higher Education of the Russian Federation, State Assignment No. FFWR-2024-0013.

Conflict of interest. The author declares that he has no conflict of interest.

REFERENCES

1. L. D. Landau and E. M. Lifshitz, *Course of Theoretical Physics*, Vol. 3: *Quantum Mechanics: Non-Relativistic Theory*, Pergamon, Oxford (1977).

2. M. J. Ablowitz and Z. H. Musslimani, *Discrete Vector Spatial Solitons in a Nonlinear Waveguide Array*, Phys. Rev. E **65**, 056618 (2002).

3. X. Luo, Q. Xie, and B. Wu, *Nonlinear Coherent Destruction of Tunneling*, Phys. Rev. A **76**, 051802 (2007).

4. F. Lederer, G. I. Stegeman, D. N. Christodoulides, G. Assanto, M. Segev, and Y. Silberberg, *Discrete Solitons in Optics*, Phys. Rep. **463**, 1 (2008).

5. A. Szameit, Y. V. Kartashov, F. Dreisow, M. Heinrich, T. Pertsch, S. Nolte, A. Tünnermann, V. A. Vysloukh, F. Lederer, and L. Torner, *Inhibition of Light Tunneling in Waveguide Arrays*, Phys. Rev. Lett. **102**, 153901 (2009).

6. S. Longhi, *Quantum-Optical Analogies Using Photonic Structures*, Laser Photonics Rev. **3**, 243 (2009).

7. I. L. Garanovich, S. Longhi, A. A. Sukhorukov, and Yu. S. Kivshar, *Light Propagation and Localization in Modulated Photonic Lattices and Waveguides*, Phys. Rep. **518**, 1 (2012).

8. R. A. Vicencio, C. Cantillano, L. Morales-Inostroza, B. Real, C. Mejía-Cortés, S. Weimann, A. Szameit, and M. I. Molina, *Observation of Localized States in Lieb Photonic Lattices*, Phys. Rev. Lett. **114**, 245503 (2015).

9. S. John, *Strong Localization of Photons in Certain Disordered Dielectric Superlattices*, Phys. Rev. Lett. **58**, 2486 (1987).

10. K. M. Ho, C. T. Chan, and C. M. Soukoulis, *Existence of a Photonic Gap in Periodic Dielectric Structures*, Phys. Rev. Lett. **65**, 3152 (1990).

11. E. Yablonovitch, T. J. Gmitter, R. D. Meade, A. M. Rappe, K. D. Brommer, and J. D. Joannopoulos, *Donor and Acceptor Modes in Photonic Band Structure*, Phys. Rev. Lett. **67**, 3380 (1991).

12. E. Yablonovitch, *Photonic Band-Gap Structures*, J. Opt. Soc. Am. B **10**, 283 (1993).

13. J. D. Joannopoulos, P. R. Villeneuve, and S. Fan, *Photonic Crystals: Putting a New Twist on Light*, Nature **386**, 143 (1997).

14. M. Bayindir, B. Temelkuran, and E. Ozbay, *Propagation of Photons by Hopping: A Waveguiding Mechanism through Localized Coupled Cavities in Three-Dimensional Photonic Crystals*, Phys. Rev. B **61**, R11855 (2000).

15. D. Brady, G. Papen, and J. E. Sipe, *Spherical Distributed Dielectric Resonators*, J. Opt. Soc. Am. B **10**, 644 (1993).

16. G. Burlak, A. Díaz-de-Anda, and A. Zamudio-Lara, *The Narrow Transmission Peaks and Field Confinement Produced by Defects in a Multilayered Microsphere*, Opt. Commun. **285**, 1542 (2012).

17. Y. García-Puente and R. Kashyap, *Spherical Bragg Resonators for Lasing Applications: A Theoretical Approach*, Opt. Express **30**, 47720 (2022).

18. Y. García-Puente, J.-J. Laurin, and R. Kashyap, *Experimental Characterization of Spherical Bragg Resonators for Electromagnetic Emission Engineering at Microwave Frequencies*, Sci. Rep. **13**, 20532 (2023).

19. L. D. Landau and E. M. Lifshitz, *Course of Theoretical Physics*, Vol. 8: *Electrodynamics of Continuous Media*, Pergamon, Oxford (1984).

20. V. P. Ruban, *Three-Dimensional Vector Tunneling of an Optical Wave in an Epsilon-Near-Zero Medium*, JETP Lett. **123**, 687 (2026).

21. V. P. Ruban, *Numerical Simulation of Light Structures in Bulk Epsilon-Near-Zero Media with Kerr Nonlinearity*, JETP Lett. **123**, 93 (2026).